PERGAMON

Organic Geochemistry 32 (2001) 647–665

Organic Geochemistry

www.elsevier.nl/locate/orggeochem

Origin of contrasting features and preservation pathways in kerogens from the Kashpir oil shales (Upper Jurassic, Russian Platform)

A. Riboulleau [a,b,*], S. Derenne [a], C. Largeau [a], F. Baudin [b]

[a] *Laboratoire de Chimie Bioorganique et Organique Physique, CNRS UMR 7573, ENSCP, 11 rue Pierre et Marie Curie, 75231 Paris Cedex 05, France*

[b] *Laboratoire de Stratigraphie, CNRS FRE 2400, UPMC, 4 place Jussieu, 75252 Paris Cedex 05, France*

Received 19 October 2000; accepted 1 February 2001
(returned to author for revision 15 December 2000)

Abstract

A kerogen, termed *aBS base*, from the Gorodische section (Russian Platform) was studied using a combination of microscopic, spectroscopic and pyrolytic methods in order to determine its chemical structure, source organisms and formation pathway(s). This kerogen was mainly formed via degradation-recondensation of phytoplanktonic material. Selective preservation and natural sulphurisation pathways only played a minor role, whereas a substantial contribution of ether linked lipids was noticed, revealing large oxygen cross-linking. Such observations allowed us to put forward, for the first time to the best of our knowledge, a substantial role for the oxidative reticulation pathway in the formation of a kerogen. Comparision with a previously studied sample from the same outcrop revealed contrasting features which reflect differences in preservation pathways triggered by different depositional conditions.

Keywords: Kashpir oil shales; Pyrolysis; FTIR; Solid state ^{13}C NMR; Melanoidins; Oxygen cross-linking; Preservation via oxidative reticulation

1. Introduction

The "Kashpir oil shale" is an organic-rich marine formation of Middle Volgian age (Late Tithonian, 140 Ma) deposited on the Russian Platform. This formation is a lateral equivalent of the Bazhenov Formation, the main source rock of the West Siberian giant oil fields, but was not buried enough for oil production. However, with a total outcropping and subcropping area of over 100,000 km^2, it represents one of the major oil shale reserves of Russia and has been mined for more than a century (Russell, 1990). The Kashpir oil shales crop out at a number of places along the Volga river and particularly near the village of Gorodische where the section is the stratotype of the Volgian stage (Fig. 1a). The Gorodische section shows a 6 m-thick black shale unit in the Middle Volgian. Rock-Eval analyses revealed very large variations in TOC (0.5–45%) and HI values (50–700 mg HC/g TOC) in this unit (Hantzpergue et al., 1998; Fig. 1b). Bioturbations are present in most parts of the black shale unit even in levels exhibiting high TOC values. We recently examined the OM-richest level of the section termed "*f top*" (Riboulleau et al., 2000). The kerogen of *f top* is characterised by a high sulphur content and microscopic, spectroscopic and pyrolytic studies indicated a major role of the so-called natural sulphurisation pathway in the formation of this especially rich level (TOC 45%). The present work deals with another level of the black shale unit from the Gorodische section, located 2.5 m below *f top*, termed "*aBS*

* Corresponding author. Tel.: +33-1-4427-6716; fax: +33-1-4325-7975.

E-mail address: riboulle@ccr.jussieu.fr (A. Riboulleau).

PII: S0146-6380(01)00017-1

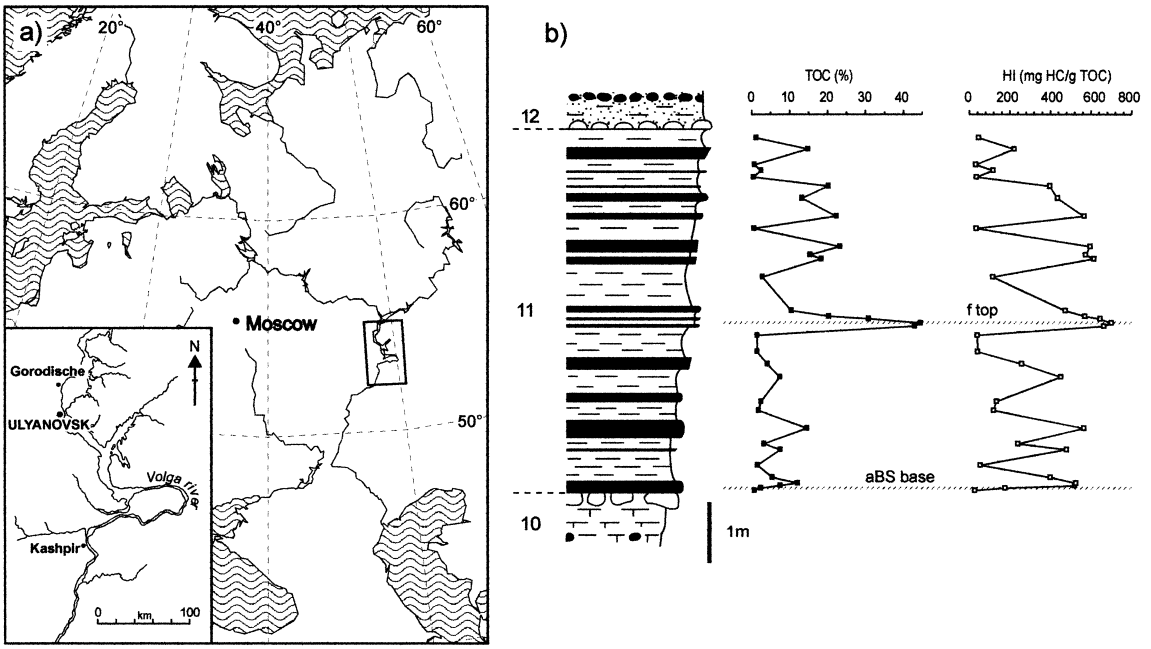

Fig. 1. (a) Location map of Gorodische outcrop. (b) Rock section of the organic-rich formation, variations of TOC and HI and location of *aBS base* and *f top* levels.

base". This level is characterised by a much lower, but still substantial, TOC content (2.3%) and exhibits intense bioturbation. As frequently observed in organic-rich formations, the Kashpir oil shales show cyclic variations in OM quality and quantity (Fig. 1b). Compared to these cyclicities, *aBS base* represents one end-member — relatively low TOC and HI — while *f top* represents the other end-member — high TOC and HI. The *aBS base* kerogen was examined by a combination of microscopic, spectroscopic and pyrolytic methods so as to derive information on its chemical structure, source organisms and formation pathway(s), and to compare the above features with those of *f top*, in order to better understand the evolution of the Russian Platform paleoenvironment.

2. Geological setting

The Gorodische outcrop is located near the city of Ulyanovsk, on the banks of the Volga river (Fig. 1a). It is mainly composed of grey clays of Middle Volgian age. A more detailed description of the section is given in Hantzpergue et al. (1998). The 6m-thick black shale unit (level 11) consists of alternating grey and black to brown clayey levels. The *aBS base* level which is studied here is a 5 cm thick bed located at the base of this organic-rich unit (Fig. 1b). Its colour is light grey and numerous shells, ammonites, bivalves, as well as bioturbations are observed.

3. Experimental

The experimental procedure is summarised in Fig. 2.

The sample was collected in 1995; a small part was ground for Rock-Eval analysis and the remainder was stored at room temperature in the dark till kerogen isolation. Rock-Eval pyrolysis (OSA device), was performed on 50 mg of finely powdered bulk rock.

For kerogen isolation, the shale was ground and extracted with $CHCl_3$/MeOH, 2:1, v/v (stirring for 12 h at room temperature) prior to the classical HCl/HF treatment (Durand and Nicaise, 1980). The kerogen concentrate thus obtained was then re-extracted under the same conditions as above.

An aliquot of the concentrate was fixed with 2% OsO_4 for electron microscopy. For transmission electron microscopy (TEM), the fixed material was embedded in Araldite, cut into ultra-thin sections and stained with uranyl acetate and lead citrate. Observations were carried out with a Philips 300 microscope. For scanning electron microscopy (SEM), the material was dehydrated using the CO_2 critical point technique and coated with gold prior to observation with a Jeol 840 microscope.

Because of the high pyrite content (ca. 30% of the concentrate), the kerogen was further purified by density fractionation (centrifugation in an aqueous solution of 71% $ZnCl_2$, $d=2.0$) prior to FTIR and ^{13}C NMR spectroscopy.

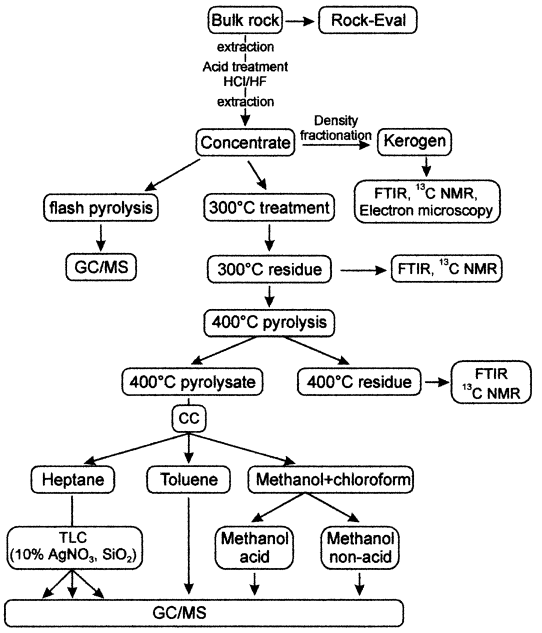

Fig. 2. Analytical procedure.

FTIR spectra of the purified kerogen were recorded on a Bruker IFS 48 spectrometer as 5 mm KBr pellets. Solid state ^{13}C NMR spectroscopy was performed on the purified kerogen with a Bruker MSL 400 spectrometer using high power decoupling, cross polarisation and magic angle spinning (CPMAS). Spectra were recorded at 3, 4 and 4.5 kHz in order to discriminate spinning side bands (SSB).

Elemental analyses of the concentrate, purified kerogen and pyrolysis residues were performed at the Service Central d'Analyse of the CNRS except the O content of the unheated kerogen concentrate which was determined by Laboratoires Wolff.

Off line pyrolysis of the concentrate was performed as described by Largeau et al. (1986). The sample was successively heated at 300°C for 20 min and 400°C for 1 h under a helium flow. The released products were trapped in cold chloroform at −5°C. After each period of heating the residue was extracted with $CHCl_3$/MeOH as described above. The first thermal treatment was aimed at eliminating thermolabile components. The 400°C pyrolysate was separated by column chromatography (Al_2O_3, act. II) into three fractions of increasing polarity, eluted with heptane, toluene and methanol, respectively. An additional elution with $CHCl_3$ was performed, yielding a small amount of products which were combined with the MeOH fraction. The heptane fraction was further fractionated into three subfractions by TLC (10% $AgNO_3$, SiO_2) developed with heptane/ether (95:5, v/v). Carboxylic acids were separated from the MeOH/$CHCl_3$ fraction using double extraction under base and acid conditions and identified as their methyl esters. Unsaturated methyl esters were identified after derivatisation with DMDS as described by Scribe et al. (1988).

All of these fractions and subfractions were analysed by GC–MS using a HP 5890 gas chromatograph (CP Sil 5 CB, 60 m fused silica capillary column, film thickness 0.4 μm, heating program 100–300°C at 4°C/min^{-1}, injector and FID at 320°C, He as carrier gas), coupled with a HP 5989 mass spectrometer with a mass range m/z = 40–600, operated at 70 eV.

Curie point pyrolysis–gas chromatography–mass spectrometry (CuPy–GC–MS) was performed on ca.1.5 mg of sample. The sample was loaded on a ferromagnetic wire with a Curie point of 610°C. The wire, placed in a glass tube, was introduced in the Curie point pyrolyser (Fisher 0316M) coupled to a Hewlett-Packard HP5890 gas chromatograph with FID (CP Sil 5 CB, 30 m fused silica capillary column, film thickness 0.4 μm, heating program from 100 to 300°C at 4°C/min; He as carrier gas). The chromatograph was coupled with a HP 5989 mass spectrometer with a mass range m/z = 40-600, operated at 70 eV.

4. Results and discussion

4.1. Bulk parameters

Rock-Eval pyrolysis of *aBS base* bulk rock showed a TOC of 2.3% and a low hydrogen index of 175 mg HC/g TOC. The low Tmax (420°C) reflects the immaturity of the sample. Elemental analyses of the kerogen concentrate displayed an H/C atomic ratio of 0.96 consistent with the low HI and a high content in heteroatoms as reflected by the O/C ratio (Table 1). High contents of total S (18.3%) and Fe (13.7%) were also noted in the concentrate. It is well documented that pyrite survives HCl/HF attacks; the iron retained in kerogen concentrates isolated by this classical treatment is therefore commonly considered to be only present as pyrite while all the non-pyritic sulphur would be organic-bound. Such a calculation indicates for *aBS base* a high percentage of pyrite (29.4%), and a rather low content of organic sulphur corresponding to a S_{org}/C ratio of only 0.026 (Table 1). Elemental analyses of the purified kerogen (Table 1), indicate a slight diminution of the ash content (24.6 vs. 30.1%), and no major change in OM composition is observed after density fractionation. A slightly higher H/C ratio is however noted (1.10); it may reflect improved accuracy of measurements due to the decrease in the mineral content. The amount of pyrite in the purified kerogen, calculated as previously described, remained fairly high (18%) indicating that the pyrite is intimately associated with the OM. Based on its bulk features, the kerogen of *aBS base* can be classified as Type II/III or altered Type II.

Table 1
Elemental analyses (wt.%) and atomic ratios of *aBS base* kerogen concentrate, *aBS base* purified kerogen and of the 300 and 400°C "off line" pyrolysis residues

	C	H	N	S_{tot}	Fe	Ashes[a]	H/C	S_{org}/C	O/C	N/C
Concentrate	38.09	3.05	0.92	18.28	13.71	30.12	0.96	0.026	0.27	0.021
Purified kerogen	44.93	4.10	1.11	12.86	8.25	24.65	1.10	0.029	—	0.021
Res 300	42.74	3.06	1.18	17.84	13.42	31.16	0.86	0.022	—	0.024
Res 400	40.05	1.53	1.22	18.77	15.89	38.48	0.46	0.006	—	0.026

[a] Almost exclusively composed of pyrite.
— not measured

4.2. Microscopic study

Under light microscopy, *aBS base* kerogen appears to be constituted chiefly of amorphous organic matter (AOM), associated with abundant pyrite. This AOM is fluffy with a dark grey to brown colour (Plate 1a) and a low contribution (ca. 5%) of gel-like orange particles. The fluffy AOM appears very spongy when observed under SEM (Plate 1b). SEM observations also showed that the pyrite occurs as both framboids and disseminated octahedron crystals. Palynomorphs are present in low amount, mostly as wood debris and dinoflagellate cysts (Plate 1c).

When examined by TEM, the AOM appears to be constituted mainly of a structureless heterogeneous organic matrix (Plate 1d). Thick cell walls (ca. 200 nm thick, Plate 1e), wood debris, homogeneous amorphous OM, and ultralaminae (thin cell walls, ca. 30 nm thick, associated into bundles, Plate 1f) are also present. The thick cell walls probably correspond to the dinoflagellate cysts observed by light microscopy and SEM, since their thickness is in the same range as that of the cyst walls observed by Kokinos et al. (1998) in a culture of the dinoflagellate *L. polyedrum*. Ultralaminae have been detected in numerous kerogens (Largeau et al., 1990), they correspond to highly resistant thin cell walls of microalgae which can retain their morphological features during kerogen formation (Tegelaar et al., 1989; Derenne et al., 1991). The occurrence of these ultralaminae reflects the selective preservation of intrinsically resistant biomolecules (algaenans) that comprise such algal walls.

Based on its microscopic features, it appears that several preservation pathways were likely implicated in the formation of *aBS base* kerogen. The presence of ultralaminae and dinoflagellate cysts reflects the involvement of the selective preservation process. However the predominant AOM reveals that one (or several) other preservation pathway(s) was (were) involved. Indeed, nanoscopic AOM in kerogen can be formed via natural sulphurisation (Boussafir et al., 1995; Mongenot et al., 1999), degradation-recondensation (Allard et al., 1997; Zegouagh et al., 1999) and/or protection by clay minerals (Salmon et al., 1997, 2000).

4.3. Spectroscopic study

The FTIR spectrum of *aBS base* kerogen is shown in Fig. 3. The weak absorptions at 2920, 2850, 1445 and 1375 cm^{-1} (CH_2 and CH_3 groups) are consistent with the low HI and H/C values of the sample. The relatively intense broad band centered at 1615 cm^{-1} points to the coexistence of olefinic and aromatic carbons in the kerogen. Oxygen-containing functions are detected as a broad band of medium intensity centred at 3400 cm^{-1} (O–H) and a band at 1700 cm^{-1} (C=O). A narrow band due to pyrite is noted at 425 cm^{-1}. The presence of this band is consistent with the substantial presence of pyrite in the purified kerogen.

The solid state ^{13}C NMR spectrum of *aBS base* kerogen (Fig. 4) shows broad peaks due to the still high abundance of pyrite retained in the purified kerogen. The spectrum is dominated by a broad peak at 30 ppm with a small shoulder at 15 ppm corresponding to CH_2 and CH_3 groups, respectively. The predominance of the 30 ppm peak suggests a relatively high aliphaticity of the kerogen which is in contrast with the low atomic H/C ratio determined by elemental analysis and FTIR data. However, as recently illustrated via examination of model compounds, solid state (CPMAS) ^{13}C-NMR can highly overestimate the aliphaticity of heterogeneous materials, due to a more efficient transfer of polarisation to protonated aliphatic carbons than to aromatic core carbons, or carbons involved in highly cross-linked structures (Poirier et al., 2000). Signals at 70, 130 and 175 ppm are noted, corresponding to C–N and/or C–O bonds, to unsaturated carbons and to C in carboxylic and/or amide groups, respectively. Signals at 210 and 170 ppm visible in Fig. 4, correspond to spinning side bands of the C=C signal, as indicated by spectra recorded at 3 and 4.5 kHz (not shown).

4.4. "Off-line" pyrolysis

4.4.1. Mass balance and elemental analysis of the residues

After heating at 300°C, the total weight loss represents ca 21% of the initial organic matter. Released products mainly correspond to volatile compounds

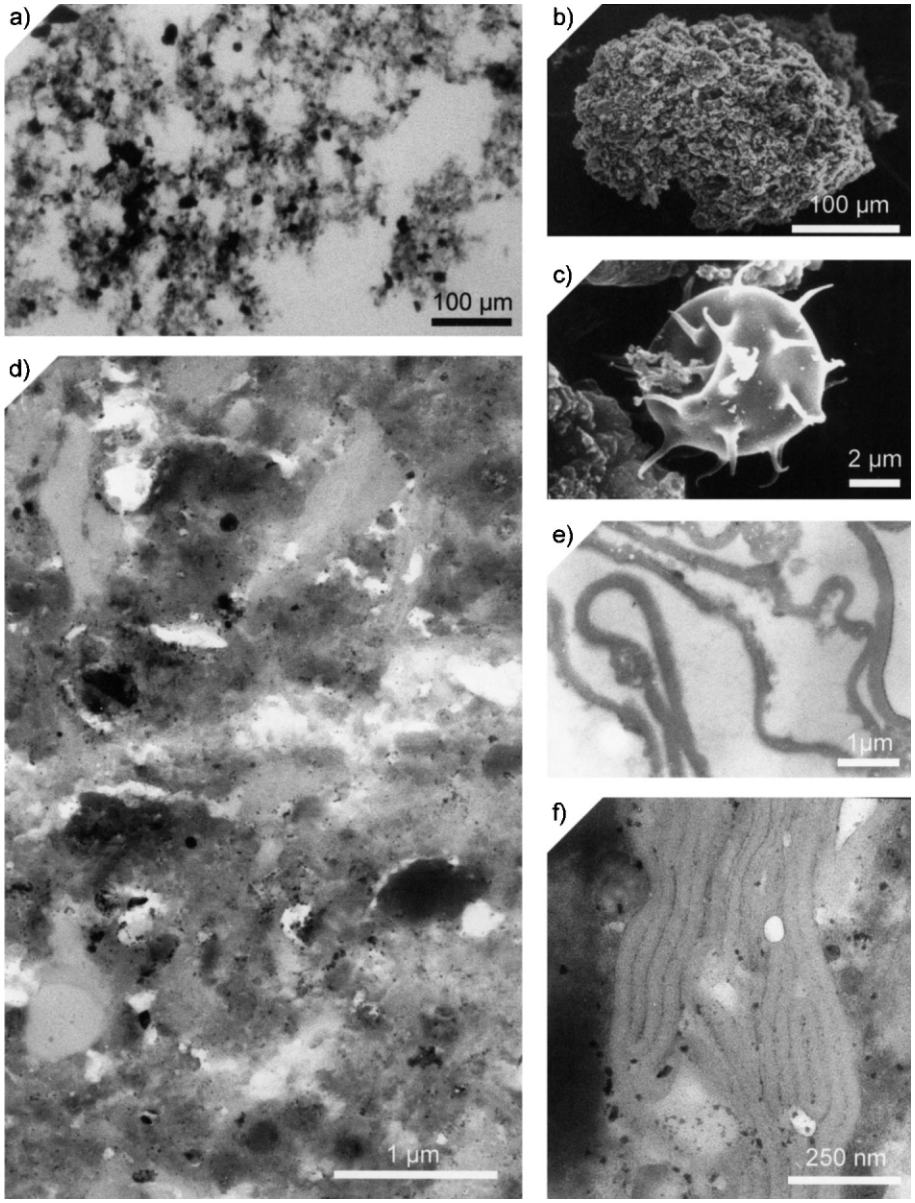

Plate 1. Microscopic observations of *aBS base* kerogen concentrate. (a) Transmitted light microscopy. (b) SEM showing a typical heterogeneous and spongy OM particle. (c) Dynoflagellate cyst observed by SEM. (d) TEM showing the dominance of the amorphous heterogeneous matrix. (e) Thick cell walls observed by TEM. (f) Detail of a bundle of ultralaminae observed by TEM.

(18% of initial OM) and the trapped compounds only represent 3% of the initial OM. After pyrolysis at 400°C, the total weight loss accounts for 34% of the initial OM. The mass of the volatile and trapped products corresponds to 20 and 14% of the unheated kerogen, respectively.

Elemental analyses of the pyrolysis residues are reported in Table 1. The H/C ratio slightly decreases upon heating at 300°C whereas a large decrease is observed after pyrolysis at 400°C. The N/C ratio increases regularly, in agreement with the results of Gillaizeau et al. (1997) and Behar et al. (2000) showing some N enrichment in kerogen pyrolysis residues. A slight decrease of the S_{org}/C ratio is observed after the first thermal treatment, while the decrease is very marked after pyrolysis at 400°C.

4.4.2. *Analysis of the 400°C pyrolysate*

The GC of the crude pyrolysate shows a large hump due to numerous coeluting products. A few resolved products

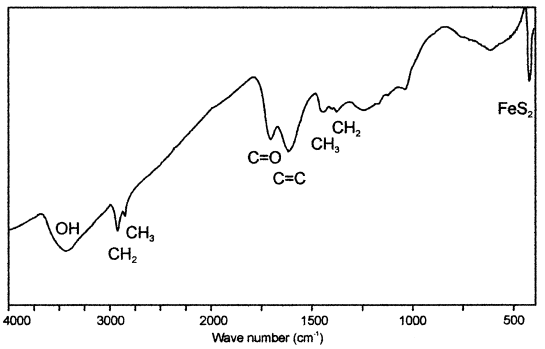

Fig. 3. FTIR spectrum of *aBS base* kerogen purified by density fractionation.

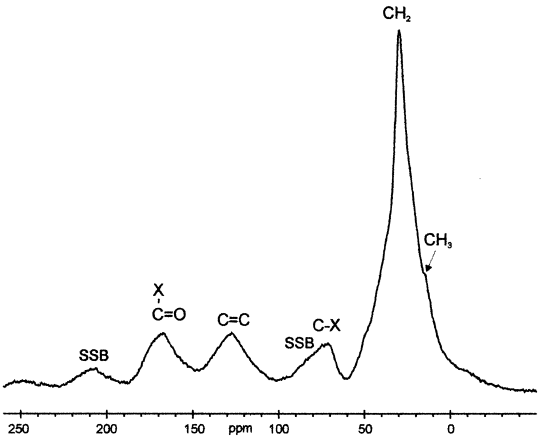

Fig. 4. Solid state CPMAS ^{13}C-NMR spectrum (4 kHz) of *aBS base* kerogen purified by density fractionation. X: N and/or O, SSB: spinning side band.

are distinguished and mainly consist of *n*-alkane/*n*-alk-1-ene doublets. The pyrolysate was therefore fractionated by column chromatography before GC/MS analyses.

4.4.2.1. Heptane-eluted fraction. This fraction represents 11% of the total pyrolysate. Its GC trace (Fig. 5) is dominated by a homologous series of *n*-alkane/*n*-alk-1-ene doublets ranging from C_{12} to C_{33} with a maximum at C_{17}. A hump of coeluting products is also present. GC/MS analysis of the subfractions obtained after $SiO_2/AgNO_3$ TLC separation of this fraction allowed the identification of a number of compounds (Table 2).

Table 2
Series of compounds identified in the heptane-eluted fraction of *aBS base* "off line" pyrolysate

Family	Ion	Range	Max
n-Alkanes	57	C_{12}–C_{33}	C_{17}
Regular isoprenoids	57	C_{15}–C_{25}	C_{18}
n-Alkylcyclohexanes	82-83	C_{13}–C_{28}	C_{19}
n-Alkylcyclopentanes	68-69	C_{13}–C_{26}	C_{20}
Dimethylalkanes	127, M^+-29	C_{19}–C_{33}	C_{23}
3-Methylalkanes	57	C_{16}–C_{30}	C_{20}
n-Alkylbenzenes	91	C_{12}–C_{30}	C_{16}
o-Methylalkylbenzenes	105	C_{13}–C_{31}	C_{16}
p-Methylalkylbenzenes	105	C_{13}–C_{30}	C_{16}
m-Methylalkylbenzenes	106	C_{13}–C_{30}	C_{16}
n-Alkyl-2-ethylbenzenes	119	C_{13}–C_{26}	C_{16}
Dimethylalkylbenzenes	119	C_{13}–C_{26}	C_{15}
Prist-2-ene	69	C_{19}	C_{19}
n-Alkylindanes	117, 131–132	C_{13}–C_{27}	C_{15},C_{16},C_{19}
2-*n*-Alkyl thiophenes	97	C_{10}–C_{27}	C_{15}
2-ω-Alkenyl thiophenes	123	C_{11}–C_{23}	C_{15}
2-*n*-Alkyl-5-methylthiophenes	111	C_{11}–C_{29}	C_{14}
2-*n*-Alkyl-5-ethylthiophenes	125	C_{11}–C_{28}	C_{15}
2-*n*-Alkyl-5-propylthiophenes	139	C_{12}–C_{25}	C_{16}
2-*n*-Alkyl-5-butylthiophenes	153	C_{13}–C_{22}	C_{16}
n-Alk-1-enes	55	C_{12}–C_{31}	C_{17}
Prist-1-ene	55	C_{19}	C_{19}
ω-Alkenylbenzenes	104	C_{12}–C_{30}	C_{30}
2-*n*-Alkylbenzothiophenes	147	C_{12}–C_{23}	C_{14}
4-*n*-Alkylbenzothiophenes	147	C_{12}–C_{23}	C_{14}
4-*n*-Alkyl-2-methylbenzothiophenes	161	C_{10}–C_{24}	C_{14}
2-*n*-Alkyl-4-methylbenzothiophenes	161	C_{10}–C_{24}	C_{14}
Alkylnaphthalenes	141	C_{10}–C_{24}	C_{15}

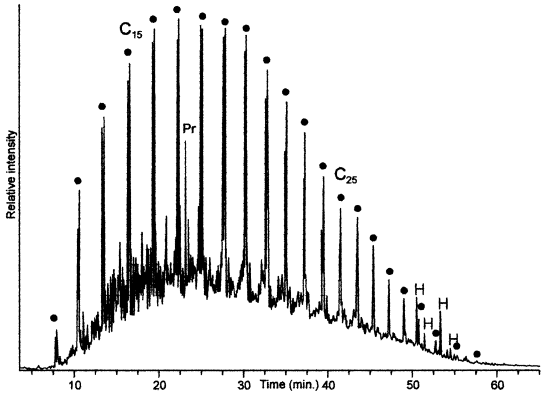

Fig. 5. GC trace of the heptane-eluted fraction of the 400°C pyrolysate of *aBS base* kerogen. ●: *n*-alkane/*n*-alk-1-ene doublets; Pr: prist-1-ene; H: hopanoids.

Besides the *n*-alkane/*n*-alkene doublets, branched and isoprenoid hydrocarbons are present in low amounts. Isoprenoids comprise regular saturated hydrocarbons from C_{15} to C_{25} (C_{17} and C_{22} missing, maximum at C_{18}), along with prist-1-ene and prist-2-ene. Such a wide range of regular saturated isoprenoids has been rarely reported in kerogen pyrolysates. C_{20}- isoprenoids are generally considered to derive from the side chain of chlorophyll a and b, α and γ tocopherols or carotenoids (see Volkman and Maxwell, 1986). The presence of longer compounds in the pyrolysate of *aBS base* attests to the presence of long isoprenoid chains in the kerogen, whose origin is unknown. Branched hydrocarbons correspond to 3-methylalkanes ranging from C_{16} to C_{30} (even-over-odd predominance) and to a series of odd carbon-numbered dimethylalkanes from C_{19} to C_{33}. The mass spectra of these dimethylalkanes indicate that methyl groups are located in position 3,7 or 3,ω–7. The

Table 3
Series of compounds identified in the toluene-eluted fraction of *aBS base* "off line" pyrolysate

Family	Ion	Range	Max
n-Alkan-2-one	58	C_9–C_{29}	C_{14}, C_{19}
n-Alkan-3-one	72	C_9–C_{29}	C_{13}, C_{15}, C_{20}
n-Alkan-4-one	86	C_9–C_{29}	C_{13}, C_{17}, C_{21}
n-Alkan-5-one	85-100	C_{10}–C_{30}	C_{18}, C_{22}
n-Alkan-6-one	99	C_{11}–C_{29}	C_{15}, C_{23}
n-Alkan-7-one	113	C_{13}–C_{27}	C_{16}, C_{24}
n-Alkan-8-one	127	C_{15}–C_{29}	C_{17}, C_{25}
n-Alkan-9-one	141	C_{17}–C_{29}	C_{18}, C_{26}
n-Alkan-10-one	155	C_{19}–C_{29}	C_{19}, C_{27}
n-Alkan-11-one	169	C_{21}–C_{28}	C_{21}, C_{28}
n-Alkan-12-one	183	C_{23}–C_{29}	C_{23}, C_{29}
n-Alkan-13-one	197	C_{25}–C_{26}	C_{26}
n-Alken-2-one	58	C_9–C_{23}	C_{13}
"*n*-Alkan-18-one"	267	C_{19}–C_{29}	C_{20}, C_{23}
3-Methyl-alkan-2-ones	72	C_{11}–C_{28}	C_{15}
Isoprenoid alkanones	58, 72	C_{18},C_{20}	—
Indanones	132 + 14n	C_{10}–C_{13}	C_{11}
1-Phenyl-alkan-1-one	105-120	C_8–C_{26}	C_{16}, C_{24}
1-Phenyl-alk-ω-en-1-one	120	C_{12}–C_{22}	C_{16}
1-(Methyl-phenyl)- alkan-1-one	119	C_{10}–C_{22}	C_{12}
1-Phenyl- alkan-2-one	119	C_{10}–C_{22}	C_{13}
Biphenyls	168 + 14n	C_{12}–C_{14}	C_{13}
Fluorenes	166 + 14n	C_{13}–C_{17}	C_{13}
Benzofluorenes	216 + 14n	C_{17}–C_{19}	C_{17}
Phenanthrenes/anthracenes	178 + 14n	C_{14}–C_{17}	C_{14}
Pyrenes	202 + 14n	C_{16}–C_{18}	—
Chrysene	228 + 14n	C_{18}–C_{20}	—
Bithiophenes	179, 193	C_9–C_{12}	C_{11}
Alkyl-phenylthiophene	160, 173	C_{11}–C_{24}	C_{11}
Methylalkyl-Phenylthiophene	187	C_{12}–C_{15}	C_{12}
Dibenzothiophenes	184 + 14n	C_{12}–C_{15}	—
Benzonitriles	117, 131	C_8–C_9	C_9
Quinolines	143 + 14n	C_{10}–C_{12}	C_{11}
Dibenzofurans	168 + 14n	C_{12}–C_{15}	C_{12}

latter series with the same pattern has been observed previously in pyrolysates of kerogens from the Kimmeridge Clay Formation (Boussafir et al., 1995), of a Toarcian kerogen from the Paris basin (Flaviano et al., 1994), of a S-rich kerogen from Orbagnoux (Mongenot et al., 1999) and in hydrogenolysis products of two Precambrian kerogens (Mycke et al., 1988). These dimethylalkanes were supposed to be of bacterial origin; however, they were also observed in the pyrolysate of the algaenan of the marine alga *Chlorella marina* (Derenne et al., 1996). Two series of *n*-alkylcycloalkanes are observed: *n*-alkylcyclohexanes and *n*-alkylcyclopentanes with a strong even-over-odd predominance ($CPI_{16-26} = 0.33$). These cyclic compounds are often observed in kerogen pyrolysates but their origin remains unclear, although thermally induced cyclisation of a linear precursor is often considered. *n*-Alkylbenzene/*n*-alk-ω-enylbenzene doublets from C_{12} to C_{30} are present together with the three methylalkylbenzene isomers, the *ortho* isomer being predominant (i.e. the one which can be formed by cyclisation and aromatisation of linear compounds). Dimethyl- and ethyl- homologues from C_{13} to C_{26} are also detected. Series of alkylindanes from C_{13} to C_{27}, and of alkylnaphthalenes from C_{10} to C_{24} are also observed. Series of hopanes and hopenes from C_{27} to C_{30}, reflecting a bacterial contribution (Rohmer et al., 1984), are observed in low amounts.

Some organic sulphur compounds (OSC) are observed in relatively low amount and are dominated by alkylated thiophenes and alkenylthiophenes from C_{10} to C_{29}. Series of alkylbenzothiophenes from C_{10} to C_{24}, and methyl homologues, are also present. The low abundance of OSC in this fraction reflects the limited involvement of natural sulphurisation, in agreement with the low S_{org}/C ratio of the kerogen.

4.4.2.2. Toluene-eluted fraction. This fraction represents 17% of the total pyrolysate. Its GC trace is relatively complex and shows an intense hump (Fig. 6a). Nevertheless, numerous series of compounds were identified via selective detection of characteristic ions (Table 3). Ketones are the main group of components in this fraction and their presence reflects the thermal cleavage of ether bridges upon pyrolysis (van de Meent et al., 1980; Largeau et al., 1986). Polyaromatic hydrocarbons and OSC occur in lower proportions. Several series of *n*-alkanones with different locations of the keto group, from C(2) to C(13) were identified in *aBS base* pyrolysate, as well as isoprenoid ketones and a series of 3-methylalkan-2-ones. The linear alkanones range from C_9 to C_{30} and present a bimodal distribution, the maximum is around C_{15} and the sub-maximum always corresponds to the compound with the carbonyl group in the C(ω-17) position (e.g. C_{23} for the *n*-alkan-6-ones) as illustrated in Fig. 6b for *n*-alkan-2-ones. The distribution of these *n*-alkan-18-ones can be observed on the ion fragmentogram

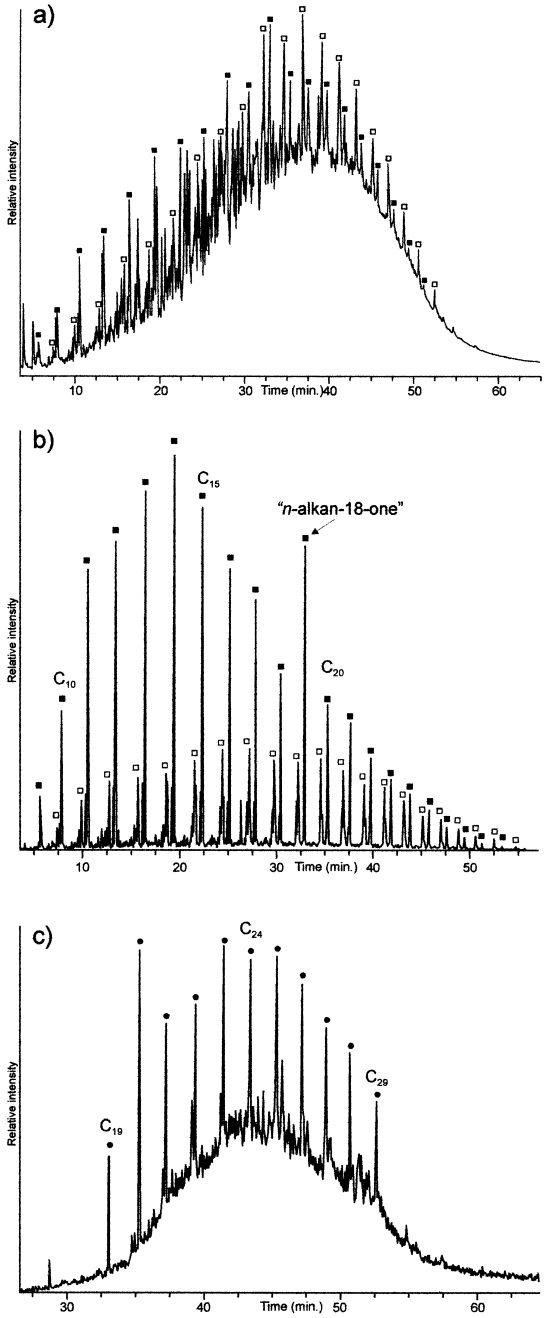

Fig. 6. (a) GC trace of the toluene eluted-fraction of the 400°C pyrolysate of *aBS base* kerogen, (b) ion chromotogram at $m/z = 58$ of the toluene-eluted fraction of the 400°C pyrolysate of *aBS base* kerogen and (c) Ion chromotogram at $m/z = 267$ of the toluene-eluted fraction of the 400°C pyrolysate of *aBS base* kerogen, showing the distribution of the "*n*-alkan-18-one" series (●). ■: *n*-alkan-2-ones, □: mid-chain *n*-alkanones.

at $m/z = 267$ corresponding to α-cleavage (Fig. 6c). The occurrence of such a variety of mid-chain ketones has previously been reported in the pyrolysates of Coorongite

(Gatellier et al., 1993), a type I kerogen from Goÿnuk (Gillaizeau et al., 1996), a Toarcian alginite from the Paris Basin (Kruge et al., 1997) and of *f top* kerogen (Riboulleau et al., 2000). This diversity should reflect cross-linking by ether bridges at various locations of the alkyl chain. However the series of *n*-alkan-18-ones indicates a preferential ether linkage at the C(18) position. Similar preferential ether linkages at specific positions on alkyl chains have been observed previously in the pyrolysates of algaenan and algaenan-derived materials: C(9) and C(10) for *botryococcus braunii*-derived kerogens and Coorongite (Gatellier et al., 1993; Sinninghe Damsté et al., 1993; Derenne et al., 1997), C(11) for the algaenan of the marine alga *Chlorella marina* (Derenne et al., 1996), C(17) and C(18) for the algaenan of the marine alga *Nannochloropsis* sp. (Gelin et al., 1996), and C(18) for a *B. braunii*-derived kerogen (Derenne et al., 1997). C_{18} and C_{20} isoprenoid alkan-2-ones (6,10,14-trimethylpentadecan - 2 - one and 3,7,11,15 - tetramethylhexadecan-2-one) are present in low amounts. The latter ketones have been observed previously in the pyrolysates of a kerogen from central Italy (Salmon et al., 1997) and of the resistant biopolymer of the L race of *Botryococcus braunii* (PRB L, Derenne et al., 1989). In both cases, these isoprenoid alkanones were very abundant in the pyrolysate and were related to dominant lycopane moieties constituting the polymer (Derenne et al., 1990a; Salmon et al., 1997). In the present case, considering the absence of other indications of a lycopane structure in *aBS base* pyrolysis products, another origin should be considered; however they are probably related to the long chain isoprenoid compounds detected in the heptane-eluted fraction. Different phenylalkanones from C_8 to C_{26}, detected using $m/z = 105 + 120$ and $91 + 119$, are present in significant amounts. Similar compounds, short chain counterparts, have been recently identified in the polar fraction of extracts of the Posidonia Shale (Wilkes et al., 1998). Note that 1-phenyl-*n*-alkan-1-ones present a second maximum at C_{24}, corresponding to the compound with a keto group on the C(ω-17) position of the alkyl chain, indicating a common precursor with the *n*-alkan-18-ones. Short chain indanones from C_{10} to C_{13} are also observed.

OSC are present in low proportion in the toluene-eluted fraction; they mostly consist of alkylphenylthiophenes, ranging from C_{11} to C_{24} detected by SID at $m/z = 173$, bithiophenes from C_9 to C_{12} (SID at $m/z = 179$) and dibenzothiophenes from C_{12} to C_{15} (SID at $m/z = 184 + 14n$).

Polyaromatic hydrocarbons are present in significant amount: including C_0–C_2 substituted biphenyls, C_0–C_4 fluorenes, C_0–C_3 phenanthrenes/anthracenes, C_0–C_2 pyrenes, C_0–C_2 benzofluorenes and C_0–C_2 chrysenes; numerous isomers are detected but no dominant polyaromatic family is noted. Polyaromatic compounds have been previously observed in large amount in the pyrolysis products of *C. marina* algaenan (Derenne et al., 1996) and in the pyrolysate of *Pediastrum*-derived Cerdanya kerogen (Sinninghe Damsté et al., 1993). Aromatic and polyaromatic nitrogen- and oxygen-containing compounds are also detected in low amount: C_8 and C_9 benzonitriles, C_{10}–C_{13} quinolines and C_{12}–C_{15} dibenzofurans.

4.4.2.3. Methanol/chloroform-eluted fraction. This fraction representing 49% of the total pyrolysate was further separated into two subfractions (acid and non-acid) by liquid/liquid extraction.

The acid subfraction (analysed as methyl esters) is dominated by saturated fatty acids from C_9 to C_{28} with a strong even-over-odd predominance ($CPI_{12\text{-}28} = 0.16$; Table 4). The major compound is *n*-C_{16}, however, *n*-C_{12}, *n*-C_{14} and *n*-C_{18} are present in relatively large amounts. Long-chain C_{20+} fatty acids only occur in low amounts, accounting for only 4% of total fatty acids. These C_{20+} acids are generally considered to originate from terrestrial material (Volkman et al., 1980; Barouxis et al., 1988). Their low relative abundance therefore indicates a low terrestrial contribution to *aBS base* kerogen, in agreement with microscopic observations. Unsaturated acids, identified after DMDS derivatisation, range from C_{14} to C_{18} and are dominated by $C_{16:1\omega10}$ and $C_{18:1\omega9}$ (oleic acid). $C_{16:1\omega10}$ is considered as a bacterial marker (Barouxis et al., 1988) whereas oleic acid is ubiquitous but considered to be mostly of phytoplanktonic origin. The other monounsaturated acids

Table 4
Fatty acid distribution in the 400°C "off line" pyrolylate of *aBS base* kerogen (% of total fatty acids detected by ion chromatography at $m/z = 74$ of the methanol-eluted acid subfraction): i, iso; ai, anteiso

	C_9	C_{10}	C_{11}	C_{12}	C_{13}	C_{14}	C_{15}	C_{16}	C_{17}	C_{18}	C_{19}	C_{20}	C_{20+}	Σ
Saturated	0.2	0.5	0.6	4.6	0.9	7.3	4.2	27	1.3	11.9	0.4	1.3	4.1	64.3
Unsaturated						1.3	1.3	11.4	0.9	11.5 di 2.9				29.3
Branched					i 0.1	i 0.6	i 0.6 ai 1.8	i 0.7	i 0.5 ai 0.6	i 0.3		i 0.3	i 0.9	6.4

are present in significantly lower proportion. $C_{18:2}$ is very common in green algae (Weete, 1976) and two isomers of this compound are observed. Unsaturated fatty acids are known to be highly sensitive to diagenetic degradation and their abundant presence (ca 30% of total fatty acids) points to a rapid and early incorporation of lipids in the kerogen. C_{13}–C_{18} branched fatty acids, generally considered as bacterial markers (Perry et al., 1979; Goossens et al., 1986), are observed in relatively low amount (6% of total fatty acids).

The methanol non-acid subfraction is dominated by two linear (C_{16} and C_{18}) alkanols, but it also exhibits a large hump due to coeluting products. The abundant presence of C_{16} and C_{18} *n*-alkanols in the non-acid subfraction of pyrolysates has previously been observed for *f top* (Riboulleau et al., 2000) and Orbagnoux (Mongenot et al., 1999) kerogens. Several other series of oxygenated compounds are detected in this subfraction among the coeluting products by selective ion detection. These series include long-chain *n*-alkylphenols ranging from C_9 to C_{23}. Such phenols have been observed previously in the pyrolysates of *f top* (Riboulleau et al., 2000), of a Cenomanian kerogen from central Italy (Salmon et al., 1997) and of Kukersite (Derenne et al., 1990b); however their origin is still unclear. Several aromatic ketones such as C_0–C_3 indanones, and C_0–C_2 tetralones are also observed. Such compounds have been recently identified in bitumens of Posidonia Shale (Wilkes et al., 1998) but their origin is unknown and they may be formed upon pyrolysis. Three series of long chain compounds, characterised by a strong peak at $m/z = 110$ and a weak molecular ion ($M^{+\bullet} = 166 + 14n$), are also detected. One of these series also shows a second peak at $m/z = 95$. According to their mass spectra, these compounds should not be isomers. Structures based on *n*-alkoxyphenol and alkylfuranone moieties are tentatively proposed for these series. Series with similar characteristics were previously observed in the pyrolysate of Cenomanian kerogens from central Italy (Salmon, 1999) and of *f top* kerogen (Riboulleau et al., 2000). Polycyclic nitrogenous compounds such as quinoline (C_9–C_{13}) and carbazole (C_{12}–C_{15}) are also detected in low amounts.

4.5. Curie point pyrolysis–gas chromatography–mass spectrometry

"Off line" pyrolysis revealed that a substantial part of *aBS base* weight loss consisted of volatile products (ca. 18% of original OM upon 300°C treatment and ca. 20% upon 400°C pyrolysis). Flash pyrolysis was, therefore, undertaken to examine the nature of these volatile products. The 610°C pyrogram of *aBS base* (Fig. 7) is dominated by a large peak of coeluting gases including CO_2 and SO_2. The abundant production of SO_2 might be related to the reaction of pyrite with the OM. In addition to long chain compounds, which were previously identified in the "off line" pyrolysate, the pyrogram shows well resolved peaks of low intensity and short retention times dominated by *n*-alkane/*n*-alk-1-ene doublets, short chain alkylbenzenes and thiophenes, and to a lesser extent short-chain alkylindanes and alkylindenes. The long chain compounds present in the flash pyrolysate were previously identified in the "off line"

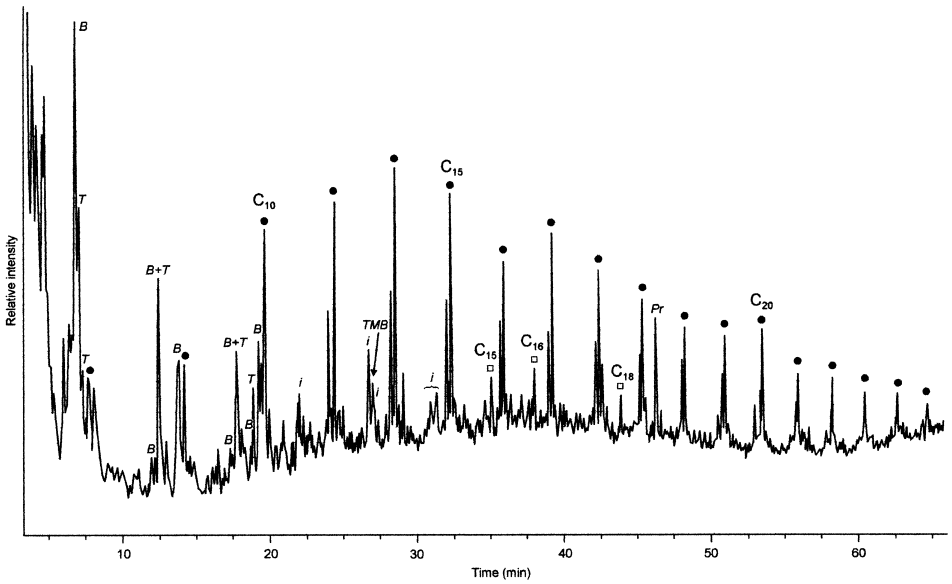

Fig. 7. Flash pyrogram at 610°C of *aBS base* kerogen. ●: *n*-alkane/*n*-alk-1-ene doublets; *T*: alkylthiophenes; *B*: alkylbenzenes; *i*: alkylindenes; *TMB*: 1,2,3,4 tetramethylbenzene; *Pr*: prist-1-ene; □: regular isoprenoids.

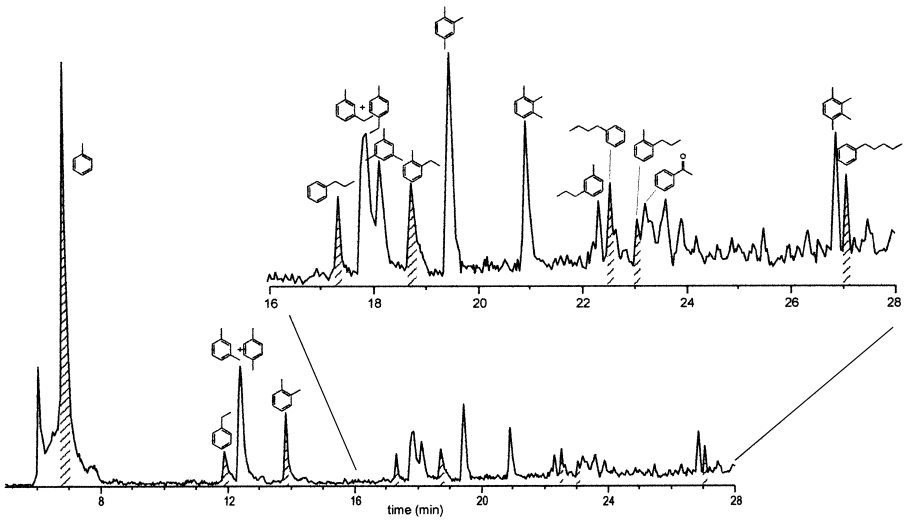

Fig. 8. Partial ion chromatogram at $m/z = 91 + 92 + 105 + 106 + 119 + 120 + 133 + 134$ showing the distribution of C_1 to C_4 alkylbenzenes in the flash pyrolysate at 610°C of *aBS base* kerogen. Acetophenone was also detected. Stripes: alkylbenzenes with a linear skeleton (*ortho* di-*n*-alkylbenzenes).

pyrolysate. The distribution and origin of these short-chain compounds is discussed below.

4.5.1. Alkylbenzenes

The distribution of C_1–C_4 alkylbenzenes is shown in Fig. 8. Toluene predominates and several isomers are detected for the short-chain compounds. Contrary to long chain counterparts, no clear dominance of compounds with a linear skeleton is noted. A substantial contribution of 1,2,3,4-tetramethylbenzene is noticed. This compound is generally considered to derive from the isorenieratene of green sulphur bacteria (Hartgers et al., 1994) but a microalgal origin was also proposed by Hoefs et al. (1995). The presence of green sulphur bacteria would indicate that anoxia extended up to the euphotic zone of the water column. Hence, a microalgal origin is more likely in the case of *aBS base* since several indications, such as intense bioturbation and abundant benthic and nectonic fauna, reveal that the water column and upper layer of the sediment were oxic during the deposition of this level.

4.5.2. Alkylthiophenes

The distribution of the short-chain alkylthiophenes, identified using mass spectra and elution times published by Sinninghe Damsté et al. (1988), is shown in Fig. 9. Such compounds are commonly found in kerogen pyrolysates. They are especially abundant in the case of S-rich kerogens (Sinninghe Damsté et al., 1988; Eglinton et al., 1992), but they are also present in the pyrolysates of S-poor kerogens (Eglinton et al., 1992; Derenne et al., 1990b; Boussafir et al., 1995). These compounds could be produced by thermal cleavage of

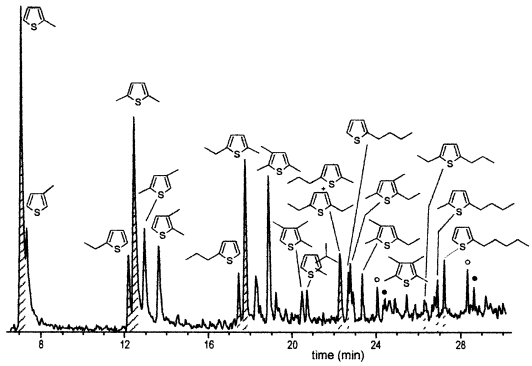

Fig. 9. Partial ion chromatogram at $m/z = 97 + 98 + 111 + 112 + 125 + 126 + 139 + 140 + 153 + 154$ showing the distribution of C_1–C_5 alkylthiophenes in the flash pyrolysate at 610°C of *aBS base* kerogen. Stripes: alkylthiophenes with a linear skeleton (2,5-di-*n*-alkylthiophenes).

long chain sulphur-containing moieties with a high degree of cross linking to the macromolecular network (Sinninghe Damsté et al., 1990). Recently, however, it was shown that short-chain S-linked moieties can be present as such in kerogens due to the sulphurisation of carbohydrates (van Kaam-Peters et al., 1998; Sinninghe Damsté et al., 1998).

The short-chain alkylthiophenes present in the *aBS base* pyrolysate are dominated by linear isomers, namely 2-*n*-alkyl- and 2-*n*-alkyl-5-methylthiophenes, which is consistent with a marine origin (Eglinton et al., 1992). However, substituted thiophenes with a non-linear skeleton are also present in significant amounts.

4.5.3. Alkylindanes and alkylindenes

Series of alkylated indanes and indenes (C_0–C_3 substituted) are detected in the *aBS base* pyrolysate in relatively low amounts. These compounds have been previously observed, with a similar distribution, in the pyrolysates of recent sediments from the northwestern Mediterranean Sea (Peulvé et al., 1996), from the north west African upwelling (Zegouagh et al., 1999) and from the Black Sea (Garcette-Lepecq et al., 2000). Their origin is, however, unknown.

4.6. Source organisms and preservation pathway(s) of aBS base kerogen

Our morphological study of *aBS base* kerogen showed that it is heterogeneous at different scales of observation. The complexity of the pyrolysis products is consistent with this heterogeneous structure. Most of the pyrolysis products, however, are based on a linear skeleton and show a distribution centred around C_{15}–C_{17}, which indicates that *aBS base* kerogen is mainly derived from algal lipids. A small contribution of bacterial lipids is also noted, from the presence of branched compounds and hopanoids in the pyrolysate. A terrestrial contribution is inferred from the microscopic observations and from the presence of C_{20+} fatty acids in the pyrolysate, but no common pyrolysis products of lignin were detected, indicating that the terrestrial contribution is small.

Based on microscopy, and chemical composition, it appears that several preservation pathways were involved in the formation of the kerogen of *aBS base*.

4.6.1. Selective preservation

The involvement of the selective preservation pathway in the formation of *aBS base* kerogen is clearly indicated by the presence of recognisable dinoflagellate cysts and ultralaminae. This is also supported by the occurrence, in the pyrolysate of *aBS base*, of characteristic pyrolysis products of algaenans from selectively preserved cell walls of algae and especially of *n*-alkanones. The series of *n*-alkan-18-ones, present in the *aBS base* pyrolysate, recalls the series of *n*-alkan-17- and-18-ones observed by Gelin et al. (1996, 1999) in the pyrolysate of algaenans from *Nannochloropsis* sp. and the *n*-alkan-18-ones observed by Derenne et al. (1997) in the pyrolysate of a *Botryococcus braunii*-derived kerogen from Hungary. We therefore consider that such alkanones are derived from selectively preserved algaenans. In addition to aliphatic compounds, aromatic compounds have been shown to be present in the pyrolysis products of intrinsically resistant cell walls of microalgae: they include alkylindanes, alkylbenzenes and phenylketones for dinoflagellate cysts (Kokinos et al., 1998) or alkylbenzenes, alkylnaphthalenes and pyrenes for *Chlorella marina* algaenan (Derenne et al., 1996). Similar aromatic compounds were identified in the pyrolysate of *aBS base*, which is consistent with the implication of the selective preservation pathway.

According to microscopic observations, dinoflagellate cysts and ultralaminae only represent a small proportion of *aBS base* kerogen. However, recently studied algaenans of the marine microalgae *C. marina* (Derenne et al., 1996) and *Nannochloropsis salina* (Gelin et al., 1999) proved them to be amorphous when observed by TEM. Such selectively preserved amorphous algaenans could contribute to the nanoscopically amorphous heterogeneous organic matter observed by TEM in *aBS base* kerogen. Several features, however, point to a minor contribution of algaenans to *aBS base* kerogen. The algaenans studied so far, structured or amorphous, have shown a very high aliphaticity as indicated by spectroscopic and pyrolytic methods as well as by high H/C ratios (Largeau et al., 1986; Derenne et al., 1996; Gelin et al., 1996); even the "aromatic" algaenan of *C. marina* exhibits an atomic H/C ratio of 1.3. Consistently, algaenan-derived kerogens are therefore characterised by high H/C ratios (e.g. Largeau et al., 1986; Derenne et al., 1991; Sinninghe Damsté et al., 1993; Gillaizeau et al., 1996). In contrast, *aBS base* kerogen exhibits a low H/C ratio of 1.10. In addition, pyrolysis of algaenan-derived kerogens yields a large amount of non-polar aliphatic compounds and the corresponding heptane-eluted fraction generally represents 40–65% of the crude pyrolysate (Derenne et al., 1991; Gillaizeau et al., 1996). The heptane-eluted fraction only accounts for 11% of the crude pyrolysate of *aBS base* kerogen, again indicating the low contribution of aliphatic compounds. Finally, no *n*-alkylnitriles, considered to be typical pyrolysis products of ultralaminae-containing kerogens (Derenne et al., 1991, 1997; Flaviano et al., 1994; Boussafir et al., 1995; Gillaizeau et al., 1996), were detected in *aBS base* pyrolysate. All these features indicate that the selective preservation pathway played only a minor role in the formation of *aBS base* kerogen. It must however be noted that, due to their low abundance in the pyrolysate, the *n*-alkane/*n*-alk-1-ene doublets might be mostly accounted for by the low proportion of algaenans selectively preserved in *aBS base* kerogen. In contrast, only a small proportion of the *n*-alkanones observed, mostly the *n*-alkan-18-ones, can be accounted for by these algaenans.

4.6.2. Natural sulphurisation

Natural suphurisation occurs in anoxic settings, where reduced sulphur produced by sulphate-reducing bacteria is abundant and Fe is low. The reaction of this reduced sulphur with OM leads to the formation of high-molecular-weight sulphur-containing compounds that exhibit a high resistance to diagenetic degradation (for a review see Sinninghe Damsté and de Leeuw,

1989). Natural sulphurisation leads to the formation of orange gel-like AOM (light microscopy) which is nanoscopically amorphous and homogeneous when observed by TEM (Boussafir et al., 1995; Mongenot et al., 1999) and is reflected by the abundance of organosulphur compounds (OSC) such as thiophenes or benzothiophenes in kerogen pyrolysates (Sinninghe Damsté et al., 1988).

Orange gel-like particles are only present in low amount (5%) in *aBS base* kerogen. Moreover OSC only represent a low proportion of the pyrolysis products, which is consistent with the low S_{org}/C ratio of the kerogen. This indicates that sulphurisation only played a minor role in the formation of *aBS base* kerogen. A relatively high rate of sulphate-reduction in the sediment is however inferred from the high pyrite content of *aBS base* concentrate (~30%). It therefore appears that only a small proportion of reduced sulphur could react with the OM, either due to the low reactivity of the latter and/or to large amounts of reactive iron in the sediment.

4.6.3. Degradation-recondensation

This process was for a long time considered as the only preservation pathway of organic matter (Tissot and Welte, 1978; Larter and Douglas, 1980). It is based on the random recombination of the monomers that are liberated by the degradation of biopolymers such as proteins and polysaccharides. This recombination leads to the formation of a highly cross-linked material that presents a melanoidin-like structure and is refractory to further degradation. Melanoidins are recondensation products of altered proteins and carbohydrates by Maillard-type reactions which may also include lipids (Larter and Douglas, 1980; Rubinsztain et al., 1986a, b). Such melanoidin-like compounds have been observed in soils (van Bergen et al., 1997), in dissolved and particulate marine organic matter (van Heemst et al., 1993; Sicre et al., 1994; Peulvé et al., 1996) and in recent sediments where they were shown to exhibit an amorphous nature at high TEM magnification (Zegouagh et al., 1999).

As indicated by its mostly amorphous nature when observed by TEM, *aBS base* kerogen could be chiefly derived from the degradation-recondensation pathway. Melanoidins are characterised by a high oxygen content and a relatively low aliphaticity (Rubinsztain et al., 1984), and so is the kerogen of *aBS base*. Moreover, the FTIR spectrum of *aBS base* kerogen is similar to melanoidin spectra previously published (Rubinsztain et al., 1986a, b; Allard et al., 1997). Finally, some of the pyrolysis products of *aBS base* kerogen such as indanes and indenes, indanones, quinolines and naphthalenes are similar to pyrolysis products of synthetic melanoidins and of melanoidin-like materials of Recent environments (Engel et al., 1986; Sicre et al., 1994; Peulvé et al., 1996). The pyrolysate of *aBS base* kerogen is however characterised by the absence of some of the typical pyrolysis products of melanoidins, i.e. short chain alkylphenols corresponding to protein-derived moieties (Boon et al., 1984; Engel et al., 1986; Zegouagh et al., 1999) and furan derivatives corresponding to polysaccharide-derived moieties (Boon et al., 1984; Saiz-Jimenez and de Leeuw, 1986). A recent study, however, demonstrated that the pyrolysis products of a 1:1 mixture of melanoidins and polyethylene, are dominated by *n*-alkane/*n*-alk-1-ene doublets and that typical pyrolysis products of melanoidins, such as phenols and furans, are almost absent (Poirier et al., 2000). Similarly, a pronounced underestimation of melanoidin-like components was also observed by these authors in the refractory organic matter isolated from a forest soil. Such a drawback is due to the very low yield of GC-amenable products generated upon pyrolysis of melanoidins and melanoidin-like materials, whereas aliphatic moieties afford very high yields. Poor detection of these types of compounds was also noted via CPMAS solid state ^{13}C NMR spectroscopy due to poor magnetisation of highly cross-linked melanoidin carbons (Poirier et al., 2000). In contrast, FTIR appeared as a relatively efficient method for the detection of such components. Melanoidin-like materials are therefore hardly detected by pyrolysis experiments and CPMAS solid state ^{13}C NMR spectroscopy in heterogeneous materials containing highly aliphatic moieties, even when the former occur in large amounts and the latter are minor components. Such a situation is encountered in *aBS base* kerogen. The microscopic and FTIR features and, to some extent, the pyrolysate composition, are consistent with a substantial contribution of melanoidin-like material formed via the degradation-recondensation pathway.

4.6.4. Oxidative reticulation

As already stressed, the kerogen of *aBS base* is characterised by a high oxygen content. However, all the oxygen functions cannot be accounted for by the presence of the above-mentioned melanoidin-like compounds. Indeed, the kerogen is characterised by abundant production of oxygen-containing compounds upon pyrolysis, especially *n*-alkanones, phenyl ketones and long chain alkyphenols, which cannot be related to melanoidin-like moieties. Normal alkanones are common pyrolysis products of algaenans (Derenne et al., 1991; Gelin et al., 1996, 1999) and derived kerogens. However such an origin cannot be considered here since (i) as discussed above, the selective preservation of algaenans only played a minor role in the formation of *aBS base* kerogen, (ii) the alkanones formed upon algaenan pyrolysis generally show a specific distribution whereas a complex mixture of isomeric alkanones with the keto group located on the C(2)–C(13) carbon atom is observed in the present case. A similar production of a large range

of alkanones was previously noted in the pyrolysates of Coorongite (Gatellier et al., 1993), of Göynük kerogen (Gillaizeau et al., 1996), of a Toarcian alginite from the Paris Basin (Kruge et al., 1997) and of *f top* kerogen (Riboulleau et al., 2000). In the case of Göynük kerogen and the Toarcian alginite, no clear origin could be determined for this wide range of alkanones. Coorongite is a rubbery material formed during blooms of *Botryococcus braunii* via drying of the algal biomass on lake shores (Dubreuil et al., 1989). Coorongite is thus exposed to strong oxidising conditions and it has been shown that the alkanones, observed in its pyrolysate, originated from the thermal cleavage of the ether bonds formed during Coorongite diagenesis via oxidative cross-linking of *B. braunii* lipids (Gatellier et al., 1993). Recent studies on S-rich kerogens and polar fractions of bitumens, also pointed to the contribution of oxygen links, in addition to those of sulphur, in the formation of the macromolecular structure (Richnow et al., 1992; Koopmans et al., 1997; Schaeffer-Reiss et al., 1998; Putschew et al., 1998; Jenisch-Anton et al., 1999). In addition, the examination of the non-polar fraction of sulphur-rich oils and sediment extracts (Jenisch-Anton et al., 1999), suggested that (i) some oxygen functions may have participated to cross-linking and (ii) oxygen and sulphur may compete at or near the oxic/anoxic interface for reaction with double bonds. Some of these unsaturated sites might be directly derived from biological lipid precursors while others would originate from diagenetic processes, including isomerisation or random migration. In the above materials, moieties could be S- and/or O- linked to the macromolecular network (Richnow et al., 1992; Koopmans et al., 1997; Schaeffer-Reiss et al., 1998; Putschew et al., 1998) and oxygen incorporation into lipids may have played a protective role, in addition to sulphur incorporation (Jenisch-Anton et al., 1999). However, in all of these S-rich materials, the proportion of oxygen incorporated via cross-linking was low. In contrast the formation of *aBS base* kerogen was only associated with a low incorporation of sulphur to the organic matter, while oxygen incorporation and cross-linking was probably a major process. This is shown by the high level of oxygen-linked moieties and, especially, the abundant production of a complex mixture of alkanones upon pyrolysis. The location of the keto group on any carbon from C(2) to C(13) should reflect diagenetic migration of double bonds that resulted in a random distribution of oxygen incorporation. Moreover, the slight preference observed in *aBS base* pyrolysate for location at the ω-17 position (the *n*-alkan-18-ones series) should reflect the additional contribution of series of alkanones derived from (i) ether bridges in the algaenans, occurring in low amount in the kerogen, and possibly (ii) oxygen incorporation in specific double bonds directly inherited from the lipids before their diagenetic randomisation. Such oxygen incorporation into specific unsaturated sites was previously observed in the case of a *Botryococcus braunii*-derived kerogen (Derenne et al., 1997) and was reflected in the presence of specific *n*-alkan-9- and-10-ones in the pyrolysate.

Such oxidative processes had been previously considered for the formation of humic and fulvic acids in the sea (Harvey et al., 1983) and could also account for the incorporation of lipids into melanoidins (Larter and Douglas, 1980). The presence of a similar mixture of ketones in the pyrolysates of other kerogens (e.g. Gillaizeau et al., 1996; Salmon et al., 1997; Riboulleau et al., 2000) suggests a common pathway of lipid preservation, via oxygen incorporation, in kerogen formation. Moreover it appears that such a pathway was especially important in the case of *aBS base* due to diagenesis under relatively oxic conditions as reflected by the intense bioturbation and well developed nectonic and benthic fauna. Such an environment is also favourable for the formation of melanoidin-like materials (van Heemst et al., 1993; Sicre et al., 1994; Peulvé et al., 1996; Zegouagh et al., 1999). Accordingly, production of melanoidin-like moieties and lipid cross-linking via oxygen incorporation were the main pathways for the formation of *aBS base* kerogen. To the best of our knowledge, this is the first time that a major role for the latter pathway has been suggested for kerogen formation.

4.7. Comparison with f top kerogen

The present study, based on microscopic, spectroscopic and pyrolytic methods, showed that *aBS base* kerogen was predominantly formed via degradation-recondensation, yielding melanoidin-like moieties and oxidative cross-linking of algal lipids. A small contribution of selectively preserved algaenan was also noted. As previously discussed, the former two processes were favoured in the well-oxygenated bottom waters, attested by the abundant bioturbation and benthic organisms present in this level. Previously studied samples from the Gorodische outcrop, *f top*, shows very different features compared to *aBS base*: this level is very organic-rich and its kerogen is highly aliphatic and was mainly formed by natural sulphurisation of lipids and carbohydrates (Riboulleau et al., 2000). The virtual absence of bioturbations and of benthic organisms in *f top* level are consistent with such a preservation pathway which needs anoxic to euxinic bottom waters (Sinninghe Damsté and de Leeuw, 1989). It therefore appears that the oxygenation level of the sediment and bottom waters changed during the deposition of the formation and strongly influenced OM preservation processes.

Despite the very different global features of *aBS base* and *f top* kerogens, their pyrolysis products exhibit a number of surprising similarities. Such similarities probably indicate that the dominant source organisms

were identical, or closely related, for the two kerogens. Major differences observed between *aBS base* and *f top* pyrolysis products are restricted to: (i) the larger proportion of sulphur-containing products in *f top* pyrolysate, (ii) the presence of algaenan-derived compounds ("*n*-alkan-18-ones") and (iii) a slightly larger proportion of bacterial markers in *aBS base* pyrolysate. Comparable observations were reported by Boussafir et al. (1995) on samples from the Kimmeridge Clay Formation. Indeed, despite contrasting bulk features, the Kimmeridge Clay kerogens showed similar pyrolysis products with similar fingerprints. Moreover, the main differences observed in the pyrolysates were the highest abundance of OSC in the pyrolysate of the OM-rich-sample and the presence of algaenan pyrolysis products (*n*-alkylnitriles) as well as bacterial lipids in the pyrolysate of the OM-poor-one (Boussafir et al., 1995). These results reflect productivity-induced changes in oxygenation conditions, attested by other studies on the Kimmeridge Clay Formation. In the case of the Kashpir oil shales, similar productivity-induced variations in oxygenation are inferred. Indeed, when the fate of sulphur is compared in the two samples, it appears, in the case of *aBS base*, that 85% of the sulphur is present as pyrite while only 10% is mineral sulphur in the case of *f top*. This indicates that during deposition of *aBS base*, enough reactive Fe was present to react with the bulk of H_2S produced by sulphate reduction while in the case of *f top*, iron was not present in sufficient amount for such reaction. The latter situation might be explained in three ways: a decrease in the proportion of Fe-bearing clay minerals due to changes in clay mineralogy, a dilution of clay minerals by carbonates or a decrease in the clay mineral/OM ratio. Changes in clay mineralogy can be observed along the Gorodische section (Chimkyavichus, 1986; Riboulleau et al., unpublished), however, such changes are not associated with large changes in a reactive Fe content. Similarly, dilution by carbonate minerals cannot be an important factor since low carbonate contents are observed along the formation. Dilution by OM should therefore account for the low relative abundance of reactive Fe in *f top* level. If we consider that the mineral flux remained relatively constant during deposition of the formation, in agreement with paleogeographic and paleoenvironmental reconstructions which indicate that sources of sediments were located far away on the platform (Thierry et al., 2000), it therefore appears that such an increase in the proportion of OM is due to an increase in phytoplankton productivity. As attested by a previous study of *f top* kerogen, this increase in OM input cannot be of terrestrial origin since the *f top* kerogen only shows a small contribution of terrestrial material (Riboulleau et al., 2000).

Fig. 10 illustrates the differences, in terms of depositional conditions, that led to the contrasting features of *aBS base* and *f top* samples. In the case of *aBS base*, relatively low primary productivity led to efficient oxidation of OM in the water column and the sediment. Only intrinsically resistant OM such as algaenans, melanoidin-like compounds and oxygen-cross-linked lipids escaped remineralisation. Oxygen consumption was however low and the oxic/anoxic interface was located in the sediment. Hydrogen sulphide, produced by OM degradation in the anoxic zone, was present in relatively low amounts and predominantly reacted with the available Fe (Fig. 10a). In contrast, very high primary productivity in the case of *f top* led to an increase in (i) oxygen consumption in the water column and (ii) sedi-

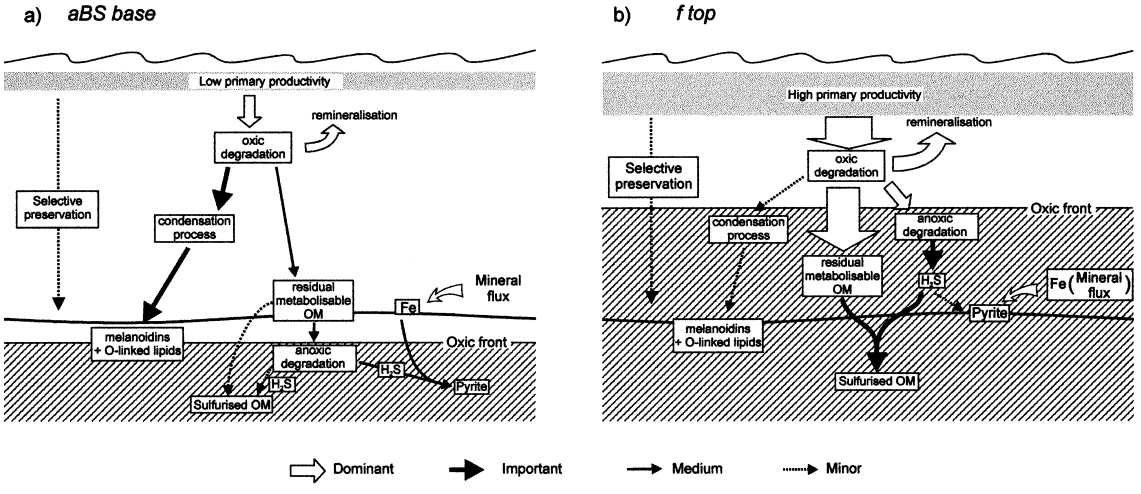

Fig. 10. Comparison of the deposition of (a) *aBS base* and (b) *f top* levels. Large differences in primary productivity during *aBS base* and *f top* depositions induced major differences in oxygenation levels of bottom waters and flux of metabolisable OM to the sediment, which resulted in large variation in the relative contribution of the different preservation pathways.

mentation rate of the OM by the formation of flocks. These changes had two important consequences firstly a rise of the oxic front above the water/sediment interface and secondly a large flux of readily metabolisable OM reached the sediment. As a result intense sulphate reduction took place. The amount of H_2S produced was very high compared to the available amount of reactive iron, so that extensive sulphurisation of the OM took place, leading to substantial preservation of the OM (Fig. 10b). Such a scenario is consistent with the very high TOC of *f top* level (45%) indicating that the sediment consisted mainly of OM; indeed, considering a C_{org}/OM mass ratio of 1.5 (elemental analysis), one can calculate that in *f top* level, OM constitutes ca. 80 vol.% of the sediment.

Primary productivity cycles are now well documented in Recent as well as in ancient marine sediments. Such cycles are due to changes in water column properties, e.g. surface temperature or mixing, and may be seasonal, annual or pluriannnal such as El Niño events or Milankovitch cycles. In the present mid-latitudes, productivity cycles are generally accompanied by a change in source organisms, such as spring diatom blooms in otherwise flagellate-dominated environments (Tyson, 1995). Similar changes in source organisms were detected in Toarcian black shales from central Italy (Bellanca et al., 1999) and were also inferred from petrographic studies of the Oxford Clay Formation (Belin and Kenig, 1994) and of the Kimmeridge Clay Formation (Pradier and Bertrand, 1992). In the latter case, such variations were confirmed by a biomarker study of bitumens (van Kaam-Peters et al., 1998). Such changes of primary producers are not observed in the present study on the basis of pyrolysis products.

Acknowledgements

CIME Jussieu for SEM observations and Mr. B. Rousseau (ENS) for preparation of ultrathin sections observed by TEM, Société de Secours des Amis des Sciences for financial support to A.R. This work is a contribution to Peri-Tethys project 95-96/28. Dr. Daniel McKinney and Pr. André Amblès are thanked for their review.

Associate Editor—**M. Vandenbroucke**

References

Allard, B., Templier, J., Largeau, C., 1997. Artifactual origin of mycobacterial bacteran. Formation of melanoidin-like artifact macromolecular material during the usual isolation process. Organic Geochemistry 26, 691–703.

Barouxis, A., Scribe, P., Dagaut, J., Saliot, A., 1988. Free and bound lipids from equatorial surficial sediments separated as a function of particle size. In: Mattavelli, L., Noveli, L. (Eds.), Advances in Organic Geochemistry 1987. Pergamon Press, Oxford. Organic Geochemistry 13, 773–783.

Behar, F., Gillaizeau, B., Derenne, S., Largeau, C., 2000. Nitrogen distribution in the pyrolysis products of a Type II kerogen (Cenomanian, Italy). Timing of molecular nitrogen production versus other gases. Energy and Fuels 14, 431–440.

Belin, S., Kenig, F., 1994. Petrographic analyses of organomineral relationships: depositional conditions af the Oxford Clay Formation (Jurassic), UK. Journal of the Geological Society, London 151, 153–160.

Bellanca, A., Masetti, D., Neri, R., Venezia, F., 1999. Geochemical and sedimentological evidence of productivity cycles recorded in Toarcian black shales from the Belluno basin, Southern Alps, Northern Italy. Journal of Sedimentary Research 69, 466–476.

van Bergen, P.F., Bull, I.D., Poulton, P.R., Evershed, R.P., 1997. Organic geochemical studies of soils from the Rothamsted Classical Experiment — I. Total lipid extracts, solvent insoluble residues and humic acids from Broadbalk Wilderness. Organic Geochemistry 26, 117–135.

Boon, J.J., de Leeuw, J.W., Rubinztain, Y., Aizenshtat, Z., Ioselis, P., Ikan, R., 1984. Thermal evaluation of some model melanoidins by Curie point pyrolysis–mass spectrometry and chromatography–mass pectrometry. Organic Geochemistry 6, 805–811.

Boussafir, M., Gelin, F., Lallier-Vergès, E., Derenne, S., Bertrand, P., Largeau, C., 1995. Electron microscopy and pyrolysis of kerogen from the Kimmeridge Clay Formation, UK: source organisms, preservation processes, and origin of the microcycles. Geochimica et Cosmochimica Acta 59, 3731–3747.

Chimkyavichus, P.I., 1986. Lithology and clay minerals of upper Jurassic deposits of the central part of East European Platform. In: Mesezhnikov, M.S. (Eds.), Jurassic Deposits of the Russian Platform. Leningrad Oil and Gas Institute, pp. 180–192 (in Russian).

Derenne, S., Largeau, C., Casadevall, E., Berkaloff, C., 1989. Occurrence of a resistant biopolymer in the L race. *Botryococcus braunii*. Phytochemistry 28, 1137–1142.

Derenne, S., Largeau, C., Casadevall, E., Sellier, N., 1990a. Direct relationship between the resistant biopolymer and the tetraterpenic hydrocarbon in the lycopadiene race of *Botryococcus braunii*. Phytochemistry 29, 2187–2192.

Derenne, S., Largeau, C., Casadevall, E., Sinningnhe Damsté, J.S., Tegelaar, E.W., de Leeuw, J.W., 1990b. Characterisation of Estonian Kukersite by spectroscopy and pyrolysis: evidence for abundant alkyl phenolic moieties in an Ordovician, Marine, type II/I kerogen. In: Durand, B., Behar, F. (Eds.), Advances in Organic Geochemistry 1989. Pergamon Press, Oxford. Organic Geochemistry 16, 873–888.

Derenne, S., Largeau, C., Casadevall, E., Berkaloff, C., Rousseau, B., 1991. Chemical evidence of kerogen formation in source rocks and oil shales via selective preservation of thin resistant outer walls of microalgae: Origin of ultralaminae. Geochimica et Cosmochimica Acta 55, 1041–1050.

Derenne, S., Largeau, C., Berkaloff, C., 1996. First example of an algaenan yeilding an aromatic-rich pyrolysate. Possible geochemical implications on marine kerogen formation. Organic Geochemistry 24, 617–627.

Derenne, S., Largeau, C., Hetényi, M., Brukner-Wein, A., Connan, J., Lugardon, B., 1997. Chemical structure of the

organic matter in a Pliocene maar-type shale: implicated *Botryococcus* race strains and formation pathways. Geochimica et Cosmochimica Acta 61, 1879–1889.

Dubreuil, C., Derenne, S., Largeau, C., Berkaloff, C., Rousseau, B., 1989. Mechanism of formation and chemical structure of Coorongite — I. Role of the resistant biopolymer and of the hydrocarbons of *Botryococcus braunii*. Ultrastructure of Coorongite and its relationship with torbanite. Organic Geochemistry 14, 543–553.

Durand, B., Nicaise, G., 1980. Procedures for kerogen isolation. In: Durand, B., (Ed.), Kerogen, pp. 33–53.

Eglinton, T.I., Sinninghe Damsté, J.S., Pool, W., de Leeuw, J.W., Eijkel, G., Boon, J.J., 1992. Organic sulphur in macromolecular sedimentary organic matter. II. Analysis of distributions of sulphur-containing pyrolysis products using multivariate techniques. Geochimica et Cosmochimica Acta 56, 1545–1560.

Engel, M.H., Rafalska-Bloch, J., Schiefelbein, C.E., Zumberge, J.E., Serban, A., 1986. Simulated diagenesis and catagenesis of marine kerogen precursors: melanoidins as model system for light hydrocarbon generation. In: Leythäuser, D., Rullkötter, J. (Eds.), Advances in Organic Geochemistry 1985. Pergamon Press, Oxford. Organic Geochemistry 10, 1073–1079.

Flaviano, C., Le Berre, F., Derenne, S., Largeau, C., Connan, J., 1994. First indication of the formation of kerogen amorphous fraction by selective preservation. Role of non-hydrolysable macromolecular constituents of Eubacterial cell wall. In: Telnæs, N., van Graas, G., Øygard, K. (Eds.), Advances in Organic Geochemistry 1993. Pergamon Press, Oxford. Organic Geochemistry 22, 759–771.

Garcette-Lepecq, A., Derenne, S., Largeau, C., Bouloubassi, I., Saliot, A., 2000. Origin and formation pathways of kerogen-like organic matter in recent sediments off the Danube Delta (northwestern Black Sea). Organic Geochemistry 31, 1663–1683.

Gatellier, J.-P.L.A., de Leeuw, J.W., Sinninghe Damsté, J.S., Derenne, S., Largeau, C., Metzger, P., 1993. A comparative study of macromolecular substances of a Coorongite and cell walls of the extant alga *Botryococcus braunii*. Geochimica et Cosmochimica Acta 57, 2053–2068.

Gelin, F., Boogers, I., Nooderloos, A.A.M., Sinninghe Damsté, J.S., Hatcher, P.G., de Leeuw, J.W., 1996. Novel, resistant microalgal polyethers: an important sink in the marine environment? Geochimica et Cosmochimica Acta 60, 1275–1280.

Gelin, F., Volkman, J.K., Largeau, C., Derenne, S., Sinninghe Damsté, J.S., de Leeuw, J.W., 1999. Distribution of aliphatic, non-hydrolyzable biopolymers in marine microalgae. Organic Geochemistry 30, 147–159.

Gillaizeau, B., Derenne, S., Largeau, C., Berkaloff, C., Rousseau, B., 1996. Source organisms and formation pathway of the kerogen of the Göynük Oil Shale (Oligocene, Turkey) as revealed by electron microscopy, spectroscopy, and pyrolysis. Organic Geochemistry 24, 671–679.

Gillaizeau, B., Behar, F., Derenne, S., Largeau, C., 1997. Nitrogen fate during maturation of a type I kerogen (Oligocene, Turkey) and related algaenans: nitrogen mass balances and timing of N_2 production versus other gases. Energy and Fuels 11, 1237–1249.

Goossens, H., Rijpstra, W.I.J., Düren, R.R., de Leeuw, J.W., 1986. Bacterial contribution to sedimentary organic matter; a comparative study of lipid moieties in bacteria and Recent sediments. In: Leythäuser, D., Rullkötter. J. (Eds.), Advances in Organic Geochemistry 1985. Pergamon Press, Oxford. Organic Geochemistry 10, 683–696.

Hantzpergue, P., Baudin, F., Mitta, V., Olferiev, A., Zakharov, V., 1998. The Upper Jurassic of the Volga basin: ammonite biostratigraphy and occurence of organic carbon-rich facies. Correlations between boreal-subboreal and submediterranean provinces. In: Crasquin-Soleau, S., Barrier, E. (Eds.), Peri-Tethys Memoir 4: Epicratonic Basins of Peri-Tethyan Platforms, pp. 9–33.

Hartgers, W.A., Sinninghe Damsté, J.S., Requejo, A.J., Allan, J., Hayes, J.M., de Leeuw, J.W., 1994. Evidence for only minor contributions from bacteria to sedimentary organic carbon. Nature 369, 224–226.

Harvey, G.R., Boran, D.A., Chesal, L.A., Tokar, J.M., 1983. The structure of marine fulvic and humic acids. Marine Chemistry 12, 119–132.

van Heemst, J.D.H., Baas, M., de Leeuw, J.W., Renner, R., 1993. Molecular characterization of marine dissolved organic matter (DOM). In: Øygard, O.K. (Ed.), Organic Geochemistry. Folch Hurtigtryhk, pp. 694–698.

Hoefs, M.J.L., van Heemst, J.D.H., Gelin, F., Koopmans, M.P., van Kaam-Peters, H.M.E., Schouten, S., de Leeuw, J.W., Sinninghe Damsté, J.S., 1995. Alternative biological sources for 1,2,3,4-tetramethylbenzene in flash pyrolysates of kerogen. Organic Geochemistry 23, 975–979.

Jenisch-Anton, A., Adam, P., Schaeffer, P., Albrecht, P., 1999. Oxygen-containing subunits in sulfur-rich nonpolar macromolecules. Geochimica et Cosmochimica Acta 63, 1059–1074.

van Kaam-Peters, H.M.E., Schouten, S., Köster, J., Sinninghe Damsté, J.S., 1998. Control on the molecular and carbon isotopic composition of organic matter deposited in a Kimmeridgian euxinic shelf sea: evidence for preservation of carbohydrates through sulfurisation. Geochimica et Cosmochimica Acta 62, 3259–3284.

Kokinos, J.P., Eglinton, T.I., Goñi, M.A., Boon, J.J., Martoglio, P.A., Anderson, D.M., 1998. Characterization of a highly resistant biomacromolecular material in the cell wall of a marine dinoflagellate resting cyst. Organic Geochemistry 28, 265–288.

Koopmans, M.P., Schaeffer-Reiss, C., de Leeuw, J.W., Lewan, M.D., Maxwell, J.R., Schaeffer, P., Sinninghe Damsté, J.S., 1997. Sulphur and oxygen sequestration of *n*-C37 and *n*-C38 unsaturated ketones in an immature kerogen and the release of their carbon skeletons during early stages of thermal maturation. Geochimica et Cosmochimica Acta 61, 2397–2408.

Kruge, M.A., Landais, P., Bensley, D.F., Stankiewicz, B.A., Elie, M., Ruau, O., 1997. Separation and artificial maturation of macerals from type II kerogen. Energy and Fuels 11, 503–514.

Largeau, C., Derenne, S., Casadevall, E., Berkaloff, C., Corolleur, M., Lugardon, B., Raynaud, J.-F., Connan, J., 1990. Occurrence and origin of ''ultralaminar structures in ''amorphous'' kerogens of various source rocks and oil shales. In: Durand, B., Behar, F., (Eds.), Advances in Organic Geochemistry 1989, Pergamon Press, Oxford. Organic Geochemistry 16, 889–895.

Largeau, C., Derenne, S., Casadevall, E., Kadouri, A., Sellier, N., 1986. Pyrolysis of immature torbanite and of the resistant

biopolymer (PRB A) isolated from extant alga *Botryococcus braunii*. Mechanism of formation and structure of torbanite. In: Leythäuser, D., Rullkötter, J. (Eds.), Advances in Organic Geochemistry 1985, Pergamon Press, Oxford. Organic Geochemistry 10, 1023–1032.

Larter, S.R., Douglas, A.G., 1980. Melanoidins-kerogen precursors geochemical lipid sinks: a study using pyrolysis gas chromatography (PGC). Geochimica et Cosmochimica Acta 44, 2087–2095.

van de Meent, D., Brown, S.C., Philp, R.P., 1980. Pyrolysis-high resolution gas chromatography and pyrolysis gas chromatography–mass spectrometry of kerogens and kerogen precursors. Geochimica et Cosmochimica Acta 44, 999–1013.

Mongenot, T., Derenne, S., Largeau, C., Tribovillard, N.-P., Lalier-Vergès, E., Dessort, D., Connan, J., 1999. Spectroscopic, kinetic and pyrolytic studies of the sulphur-rich Orbagnoux deposit (Upper Kimmeridgian, Jura). Organic Geochemistry 30, 39–56.

Mycke, B., Michaelis, W., Degens, E.T., 1988. Biomarkers in sedimentary sulfides of Precambrian age. In: Mattavelli, L., Novelli, L. (Eds.), Advances in Organic Geochemistry 1987, Pergamon Press, Oxford. Organic Geochemistry 13, 619–625.

Perry, G.J., Volkman, J.K., Johns, R.B., 1979. Fatty acids of bacterial origin in contemporary marine sediments. Geochimica et Cosmochimica Acta 43, 1715–1725.

Peulvé, S., de Leeuw, J.W., Sicre, M.-A., Baas, M., Saliot, A., 1996. Characterization of macromolecular organic matter in sediment traps from the northwestern Mediterranean Sea. Geochimica et Cosmochimica Acta 60, 1239–1259.

Poirier, N., Derenne, S., Rouzaud, J.-N., Largeau, C., Mariotti, A., Balesdent, G., Maquet, J., 2000. Chemical structure and sources of the macromolecular, resistant, organic fraction isolated from a forest soil (Lacadée, South-west France). Organic Geochemistry 31, 813–827.

Pradier, B., Bertrand, P., 1992. Etude à haute résolution d'un cycle de carbone organique de roche-mère du Kimmeridgien du Yorkshire (G.B.): relation entre composition pétrographique du contenu organique observé in situ, teneur en carbone organique et qualité pétroligène. Comptes Rendus de l'Académie des Sciences, Série II 315, 187–192.

Putschew, A., Schaeffer-Reiss, C., Schaeffer, P., Koopmans, M.P., de Leeuw, J.W., Lewan, M.D., Sinninghe Damsté, J.S., Maxwell, J.R., 1998. Release of sulfur- and oxygen-bound components from a sulfur-rich kerogen during simulated maturation by hydrous pyrolysis. Organic Geochemistry 29, 1875–1890.

Riboulleau, A., Derenne, S., Sarret, G., Largeau, C., Baudin, F., Connan, J., 2000. Pyrolytic and spectroscopic study of sulphur-rich kerogen from the "Kashpir oil shales" (Upper Jurassic; Russian Platform). Organic Geochemistry 31, 1641–1661.

Richnow, H.H., Jenisch, A., Michaelis, W., 1992. Structural investigations of sulfur-rich macromolecular oil fractions and a kerogen by sequential chemical degradation. In: Eckardt, C.B., Maxwell, J.R., Larter, S.R., Manning, D.A.C. (Eds.), Advances in Organic Geochemistry 1991, Pergamon Press, Oxford. Organic Geochemistry 19, 351–370.

Rohmer, M., Bouvier-Nave, P., Ourisson, G., 1984. Distribution of hopanoid triterpenes in procaryotes. Journal of General Microbiology 130, 1137–1150.

Rubinztain, Y., Ioselis, P., Ikan, R., Aizenshtat, Z., 1984. Investigations on the structural units of melanoidins. Organic Geochemistry 6, 791–804.

Rubinztain, Y., Yariz, S., Ioselis, P., Aizenshtat, Z., Ikan, R., 1986a. Characterization of melanoidins by IR spectroscopy — I. Galactose-glycine melanoidins. Organic Geochemistry 9, 117–125.

Rubinztain, Y., Yariz, S., Ioselis, P., Aizenshtat, Z., Ikan, R., 1986b. Characterization of melanoidins by IR spectroscopy-II. Melanoidins of galactose with arginine, isoleucine, lysine and valine. Organic Geochemistry 9, 371–374.

Russell, P.L., 1990. Oil Shales of the World, their Origin, Occurence and Exploitation. Pergamon Press, New York (754 p).

Saiz-Jimenez, C., de Leeuw, J.W., 1986. Chemical characterization of soil organic matter fractions by analytical pyrolysis–gas chromatography–mass spectrometry. Journal of Analytical and Applied Pyrolysis 9, 99–119.

Salmon, V., Derenne, S., Largeau, C., Beaudoin, B., Bardoux, G., Mariotti, A., 1997. Kerogen chemical structure and organisms in a Cenomanian organic-rich black shale (Central Italy) — indications for an important role of the "sorptive protection" pathway. Organic Geochemistry 27, 423–438.

Salmon, V., 1999. Modes d'accumulation de la matière organique dans des "black shales" et des silex du cénomanien d'Italie centrale. Rôle des minéraux et des processus diagénétiques. PhD thesis, E.N.S.M.P. Mémoire des Sciences de la Terre no. 37.

Salmon, V., Derenne, S., Lallier-Vergès, E., Largeau, C., Beaudoin, B., 2000. Protection of organic matter by mineral matrix in a Cenomanian black shale. Organic Geochemistry 31, 463–474.

Schaeffer-Reiss, C., Schaeffer, P., Putschew, A., Maxwell, J.R., 1998. Stepwise chemical degradation of immature S-rich kerogens from Vena del Gesso (Italy). Organic Geochemistry 29, 1857–1874.

Scribe, P., Guezennec, J., Dagaut, J., Pepe, C., Saliot, A., 1988. Identification of the position and the stereochemistry of the double bond in monounsaturated fatty acid methyl esters by gas chromatography/mass spectrometry of dimethyl disulfide derivatives. Analytical Chemistry 60, 928–931.

Sicre, M.-A., Peulvé, S., Saliot, A., de Leeuw, J.W., Baas, M., 1994. Molecular characterization of the organic fraction of suspended matter in the surface waters and bottom nepheloid layer of the Rhone delta using analytical pyrolysis. Organic Geochemistry 21, 11–26.

Sinninghe Damsté, J.S., Kock-van Dalen, A.C., de Leeuw, J.W., Schenck, P.A., 1988. Identification of homologous series of alkylated thiophenes, thiolanes, thianes and benzothiophenes present in pyrolysates of sulphur-rich kerogens. Journal of Chromatography 435, 435–452.

Sinninghe Damsté, J.S., de Leeuw, J.W., 1989. Analysis, structure and geochemical significance of organical-bound sulphur in the geosphere: state of the art and future research. Organic Geochemistry 16, 1077–1101.

Sinninghe Damsté, J.S., Eglinton, T.I., Rijpstra, W.I.C., de Leeuw, J.W. 1990. Characterization of organically bound sulfur in high-molecular-weight, sedimentary organic matter using flash pyrolysis and Raney Ni desulfurization. In: Orr, W.L., White, C.M. (Eds.), Geochemistry of Sulfur in Fossil Fuels. American Chemical Society Symposium Series 429, American Chemical Society, Washington, pp. 486–528.

Sinninghe Damsté, J.S., de las Heras, F.X.C., van Bergen, P., de Leeuw, J.W., 1993. Characterization of Tertiary Catalan lacustrine oil shales: discovery of extremely organic sulphur-rich Type I kerogens. Geochimica et Cosmochimica Acta 57, 389–415.

Sinninghe Damsté, J.S., Kohnen, M.E.L., Horsfield, B., 1998. Origin of low-molecular-weight alkylthiophenes in pyrolysates of sulphur-rich kerogens as revealed by micro scale scealed vessel pyrolysis. Organic Geochemistry 29, 1891–1903.

Tegelaar, E.W., de Leeuw, J.W., Derenne, S., Largeau, C., 1989. A reappraisal of kerogen formation. Geochimica et Cosmochimica Acta 53, 3103–3106.

Thierry, J. et al. (41 co-authors), 2000. Early Tithonian. In: Dercourt, J., Gaetani, M. et al. (Eds.), Atlas Peri-Tethys, Palaeogeographical Maps. CCGM/CGMW, Paris, map 11.

Tissot, B.P., Welte, D.H., 1978. Petroleum Formation and Occurrence. Springer-Verlag, Berlin, 538 p.

Tyson, R.V., 1995. Sedimentary Organic Matter. Chapman & Hall, London, 616 p.

Volkman, J.K., Maxwell, J.R., 1986. Acyclic isoprenoids as biological markers. In: Johns, R.B. (Ed.), Biological Markers in the Sedimentary Record. Elsevier, Amsterdam, pp. 1–42.

Volkman, J.K., Johns, R.B., Gillan, F.T., Perry, G.J., 1980. Microbial lipids of an intertidal sediment — I. Fatty acids and hydrocarbons. Geochimica et Cosmochimica Acta 44, 1133–1143.

Weete, J.D., 1976. Algal and fungal waxes. In: Kolattukudy, P.E. (Ed.), Chemistry and Biochemistry of Natural Waxes. Elsevier, Amsterdam, pp. 349–418.

Wilkes, H., Disko, U., Horsfield, B., 1998. Aromatic aldehydes and ketones in the Posidonia Shale, Hils syncline, Germany. Organic Geochemistry 29, 107–117.

Zegouagh, Y., Derenne, S., Largeau, C., Bertrand, P., Sicre, M.-A., Saliot, A., Rousseau, B., 1999. Refractory organic matter in sediments from the North-West African upwelling system: abundance, chemical structure and origin. Organic Geochemistry 30, 101–118.